# Supporting Information

**Aza-bodipy Dyes with Heterocyclic Substituents and Derivatives Bearing Cyanide Co-Ligand: NIR Absorbing Materials for Vacuum-processed BHJ Solar Cells**

**Content**

## Experimental section

### General

Starting materials were purchased from commercial sources and used without further purification. The solvents THF and DCM were extra dry obtained from Acros. Diethyl ether was dried over sodium and distilled freshly before use. $^{1}$HNMR and $^{13}$CNMR spectra were recorded on a Bruker DRX 500 P instrument and $^{19}$FNMR were recorded on a Bruker Avance 300 instrument. Mass spectra were measured on a Bruker Esquire-LC 00084 instrument as DCM solutions. Melting points were determined with a Netzsch STA 449C instrument. The UV-vis absorption spectra were obtained on a Perkin Elmer λ 25 spectrometer for solution samples and a Shimadzu Solidspec-3700 UV-vis-NIR spectrophotometer was used to record absorption spectra for thin film samples. The emission spectra were measured with an Edinburgh Instruments spectrometer as DCM solutions. Thermal properties, including TGA, DTA and DSC were measured on Netzsch STA 449C under argon atmosphere with the heating rate of 10 K min$^{-1}$. Cyclic voltammetry measurements were carried out with a Metrohm μ-Autolab instrument in a single-component cell under nitrogen. A typical three electrode system with a platinum disk working electrode, a platinum wire counter electrode and a silver rod coated electrochemically with AgCl reference electrode was employed. The potentials were measured versus Ag/AgCl and referenced to ferrocene as an internal standard ($E_{Fc/Fc^+}$ = –4.78 eV). The measurements were conducted with a scan rate of 100 mV s$^{-1}$ in degassed HPLC grade DCM containing tetra-*n*-butylammonium hexafluorophosphate (TBAHFP, 0.1 M) as supporting electrolyte.

### X-ray single crystal diffraction

Suitable single crystal sample was mounted on a glass fibre with two-component glue. Data were collected using a Bruker SMART APEX2 area detector diffractometer equipped with an Oxford Cryosystems low-temperature apparatus operating at T = 200 K. Data were measured using Mo Kα radiation (sealed X-ray tube, 50 kV, 30 mA). The total number of runs and images was based on the strategy calculation from the program APEX2 (Bruker). Cell parameters were retrieved using the SAINT (Bruker, V8.34A, 2013) software and refined using SAINT (Bruker, V8.34A, 2013). Data reduction was performed using the SAINT (Bruker, V8.34A, 2013) software which corrects for Lorentz polarisation. The structure was solved by Direct Methods using the ShelXT (Sheldrick, 2015) structure solution program and refined by Least Squares using version 2013-4 of ShelXL (Sheldrick, 2008). All non-hydrogen atoms were refined anisotropically. Hydrogen atom positions were calculated geometrically and refined using the riding model.

### Theoretical calculation

The density functional theory (DFT) calculations are carried out with Gaussian 09 software package. The ground state geometry of all the compounds are fully optimized with the B3LYP exchange-correlation functional and 6–31G** basis set is applied for all the atoms. Vibrational frequency calculations are performed at the same time to validate that the obtained structures are minima on potential energy surface. In order to reproduce the real situation, solvent effect is taken into consideration by using C-PCM solvent model as in DCM solutions.

### Syntheses and characterizations

*N-methyl-pyrrolyllithium*: 4.8 ml 2.5 M n-butyl lithium in hexane (1.0 equiv) was added dropwise

into the vigorously stirring anhydrous THF solution (15 ml) of 12.0 mmol *N*-methylpyrrole (0.97 g) at –78℃. The system turned from light yellow into an orange clear solution. The solution of *N*-methyl-pyrrolyllithium was allowed to warm to room temperature (around 20℃) and stirred for another 2 h. This solution of *N*-methyl-pyrrolyllithium was used in the following reactions without further purifications or characterizations.

*N-methyl-indolyllithium*: 4.8 ml 2.5 M n-butyl lithium in hexane (1.0 equiv) was added dropwise into the vigorously stirring anhydrous THF solution (15 ml) of 12.0 mmol *N*-methylindole (1.57 g) at –78℃. Then, the solution of *N*-methyl-indolyllithium was allowed to warm to room temperature (around 20℃) and stirred for another 2 h. The system turned from a light yellow clear solution into a dark yellow suspension. This suspension of 1-methyl-indolyllithium was used in the following reactions without further purifications or characterizations.

*5-(trimethylsilyl)thienyllitium*: 4.8 ml 2.5 M n-butyl lithium in hexane (1.0 equiv) was added dropwise into the vigorously stirring anhydrous ether solution (40 ml) of 12.0 mmol 2-(trimethylsilyl)thiophene (1.87 g) at –78℃. The solution of 5-(trimethylsilyl)thienyllitium was allowed to warm to room temperature (around 20℃) and stirred for another 2 h. The system turned from light yellow into a yellow clear solution. This solution of 5-(trimethylsilyl)thienyllitium was used in the following reactions without further purifications or characterizations.

*General synthesis of aza-diisoindolmethine*: An organolithium reagent (1.2 equiv) in THF and hexane was added dropwise into a vigorously stirred suspension of phthalodinitrile (10.0 mmol) in diethyl ether (40 ml) at –70℃ under nitrogen. After complete addition, the system was allowed to warm up to room temperature and stirred for another 3 h. The solvent was removed in vacuum and 50 ml formamide was added into the dark reaction mixture. The system was heated rapidly to reflux (around 210 ℃) and a coppery shiny precipitate formed with $NH_3$ gas given out. After the system was cooled to room temperature, the precipitate was filtered and washed with methanol/water (5×30 ml, v/v=2:1). Flash chromatography was performed to give the aza-diisoindolmethine precursors as metalescent solids.

**1a**: Dark blue solid, 0.31 g (0.77 mmol), yield 15%. Eluent (acetone/hexane=1:10, v/v). $^1$H NMR (600 MHz, $CDCl_3$) δ 12.70 (s, 1H), 8.11 (d, $J$ = 7.9 Hz, 2H), 7.74 (d, $J$ = 8.0 Hz, 2H), 7.37 (t, $J$ = 7.2 Hz, 2H), 7.28 (t, $J$ = 7.4 Hz, 2H), 6.89 (d, $J$ = 47.3 Hz, 4H), 6.35 (dd, $J$ = 3.7, 2.7 Hz, 2H), 3.96 (s, 6H). ESI-MS *m*/*z* calculated for $[C_{26}H_{22}N_5]^+$ 404.5, found 404.4.

**2a**: Dark brown solid, 0.31 g (0.61 mmol), yield 12%. Eluent (DCM/n-hexane=1:3, v/v). $^1$H NMR (300 MHz, DMSO) δ 12.90 (s, 1H), 8.18 (d, $J$ = 7.4 Hz, 2H), 8.04 (d, $J$ = 8.0 Hz, 2H), 7.76 (d, $J$ = 7.8 Hz, 2H), 7.65 (d, $J$ = 8.3 Hz, 2H), 7.53 (t, $J$ = 7.0 Hz, 2H), 7.50 – 7.40 (m, 4H), 7.35 (t, $J$ = 7.2 Hz, 2H), 7.19 (t, $J$ = 7.2 Hz, 2H), 4.14 (s, 6H). ESI-MS *m*/*z* calculated for $[C_{34}H_{26}N_5]^+$ 504.6, found 504.6.

**3a**: Dark green solid, 0.50 g (0.90 mmol), yield 18%. Eluent (DCM/n-hexane=1:3, v/v). $^1$H NMR (500 MHz, CDCl3) δ 8.09 (d, J = 7.8 Hz, 2H), 8.00 (d, J = 7.9 Hz, 2H), 7.91 (d, J = 3.5 Hz, 2H), 7.40 (t, J = 7.3 Hz, 2H), 7.35 (dd, J = 7.3, 5.4 Hz, 4H), 0.43 (s, 18H). ESI-MS *m*/*z* calculated for $[C_{30}H_{32}N_3S_2Si_2]^+$ 554.9, found 554.5.

*General synthesis of aza-BODIPY dyes*: The corresponding aza-diisoindolmethine precursor (1 mmol) was dissolved in 30 ml dry DCM and 10 equiv anhydrous DIPEA (*N*,*N*-diisopropylethylamine, 10 mmol, 1.29 g, 1.74 ml) was added dropwise at room temperature. After 1 h, 10 equiv $BF_3$•$OEt_2$ (10 mmol, 1.42 g, 1.26 ml) was added dropwise into the system at room temperature. The reaction mixture was stirred overnight. After the total conversion of the precursor

(monitored by TLC, DCM/hexane=1:1, v/v), the reaction mixture was purred into 50 ml brine and extracted by 3×100 ml DCM. The organic layers were collected and dried under reduced pressure. A short column chromatography (eluent: DCM/hexane=1/1, v/v) was performed to give the final product as metalescent powder.

**1b**: Dark purple solid, 0.28 g, yield 62%. Melting point 260 ℃. $^{1}$H NMR (500 MHz, $CDCl_3$) δ 8.10 (d, *J* = 8.2 Hz, 2H), 7.51 – 7.44 (m, 4H), 7.31 (t, *J* = 7.5 Hz, 2H), 6.94 (s, 2H), 6.90 (s, 2H), 6.33 (dd, *J* = 3.7, 2.8 Hz, 2H), 3.64 (s, 6H). $^{13}$C NMR (126 MHz, CDCl3) δ 143.10, 139.71, 133.02, 131.45, 129.78, 128.46, 126.85, 124.42, 124.06, 121.26, 117.70, 110.18, 35.93. $^{19}$F NMR (282 MHz, CDCl3) δ -115.97 (s), -133.80 (s), -151.57 (s). ESI-MS *m*/*z* calculated for $[C_{26}H_{21}BF_2N_5]^+$ 452.2, found 452.4.

**2b**: Dark red solid, 0.37 g, yield 68%. Melting point 315 ℃. $^{1}$H NMR (500 MHz, $CDCl_3$) δ 8.21 – 8.12 (m, 2H), 7.72 (d, *J* = 7.7 Hz, 1H), 7.64 (d, *J* = 7.8 Hz, 1H), 7.53 (dd, *J* = 13.2, 7.6 Hz, 4H), 7.35 (tt, *J* = 15.8, 8.1 Hz, 6H), 7.24 (s, 2H), 7.15 (t, *J* = 7.0 Hz, 2H), 3.72 (d, *J* = 41.4 Hz, 6H). $^{13}$C NMR (126 MHz, $CDCl_3$) δ 143.21, 140.70, 140.56, 133.22, 133.10, 131.84, 131.79, 130.36, 130.26, 128.20, 127.51, 124.27, 124.18, 122.30, 121.47, 120.61, 111.38, 110.13, 110.00, 32.95, 32.80. $^{19}$F NMR (282 MHz, $CDCl_3$) δ -114.99 – -116.60 (m), -132.26 (dd, *J* = 57.7, 28.9 Hz), -149.65 – -150.87 (m). ESI-MS *m*/*z* calculated for $[C_{34}H_{25}BF_2N_5]^+$ 552.4, found 552.5.

**3b**: Dark blue solid, 0.34 g, yield 56%. Melting point 201 ℃. $^{1}$H NMR (500 MHz, $CDCl_3$) δ 8.40 (d, *J* = 3.7 Hz, 2H), 8.14 (d, *J* = 8.2 Hz, 2H), 8.04 (d, *J* = 7.9 Hz, 2H), 7.46 (d, *J* = 3.7 Hz, 2H), 7.45 – 7.40 (m, 2H), 7.36 – 7.30 (m, 2H), 0.46 (s, 18H). $^{13}$C NMR (126 MHz, $CDCl_3$) δ 147.87, 143.66, 140.43, 137.02, 135.61, 134.19, 133.21, 131.09, 129.80, 127.34, 124.48, 121.25, -0.15. $^{19}$F NMR (282 MHz, $CDCl_3$) δ -134.35 – -135.11 (m). ESI-MS *m*/*z* calculated for $[C_{30}H_{31}BF_2N_3S_2Si_2]^+$602.7, found 602.5.

*General synthesis of aza-BODIPY derivatives with CN group*: The corresponding aza-bodipy dyes (1 mmol) was dissolved in 20 ml of dry DCM. Aluminum chloride (2 mmol, 0.27 g) was added and the system was heated to around 40 ℃ for 10 min. The system turned from dark green into dark brown. Trimethylsilyl cyanide (10 mmol, 1.00 g) was added dropwise and the color of the solution turned from dark brown into yellowish green. After the complete conversion of aza-bodipy dyes (monitored by TLC, DCM/hexane=2:1, v/v) in 1 h, the solution was washed with brine and the organic layer was collected and dried in vacuum. Rapid column chromatography was performed (eluent: DCM/hexane=2/1, v/v) to give the final product as metalescent powder.

**1c**: Dark purple solid, 0.30 g, yield 65%. Melting point 245 ℃. $^{1}$H NMR (500 MHz, $CDCl_3$) δ 8.12 (d, *J* = 8.2 Hz, 2H), 7.52 (t, *J* = 7.1 Hz, 4H), 7.36 (t, *J* = 7.4 Hz, 2H), 7.02 (s, 4H), 6.45 – 6.37 (m, 2H), 3.62 (s, 6H). $^{13}$C NMR (126 MHz, $CDCl_3$) δ 143.92, 138.44, 132.71, 131.10, 130.98， 130.27, 129.54, 127.29, 124.02, 123.38, 121.37, 120.63, 110.61, 35.96. $^{19}$F NMR (282 MHz, $CDCl_3$) δ -123.27 (s), -142.07 (s). ESI-MS *m*/*z* calculated for $[C_{27}H_{21}BFN_6]^+$ 459.3, found 459.3.

**2c**: Dark brown solid, 0.39 g, yield 70%. Melting point 279 ℃. $^{1}$H NMR (500 MHz, $CDCl_3$) δ 8.18 (dd, *J* = 13.1, 5.7 Hz, 2H), 7.72 (dd, *J* = 52.2, 7.8 Hz, 2H), 7.64 – 7.48 (m, 4H), 7.48 – 7.34 (m, 6H), 7.34 – 7.29 (m, 2H), 7.17 (dd, *J* = 14.9, 8.0 Hz, 2H), 3.68 (dd, *J* = 37.2, 28.7 Hz, 6H). $^{13}$C NMR (126 MHz, $CDCl_3$) δ 145.90, 144.95, 144.01, 141.16, 140.09, 139.26, 138.44, 138.32, 132.87, 132.76, 132.40, 132.16, 131.49, 130.73, 129.43, 128.36, 128.25, 127.96, 127.52, 124.89, 124.17, 123.97, 122.64, 121.57, 121.42, 120.99, 120.87, 113.99, 113.89, 111.87, 110.17, 109.98, 32.82, 32.28.$^{19}$F NMR (282 MHz, $CDCl_3$) δ -122.98 (dd, *J* = 88.5, 43.5 Hz), -142.99 (dd, *J* = 91.0, 43.8 Hz). ESI-MS *m*/*z* calculated for $[C_{35}H_{25}BFN_6]^+$ 559.4, found 559.5.

**3c**: Dark green solid, 0.41 g, yield 68%. Melting point 234 ℃. $^{1}$H NMR (500 MHz, $CDCl_3$) δ 8.30 (dd, *J* = 3.8, 0.7 Hz, 2H), 8.16 (d, *J* = 8.2 Hz, 2H), 8.08 (d, *J* = 8.0 Hz, 2H), 7.53 – 7.47 (m, 4H), 7.40 (ddd, *J* = 8.0, 7.0, 0.9 Hz, 2H), 0.43 (s, 9H). $^{13}$C NMR (126 MHz, $CDCl_3$) δ 149.43, 144.81, 139.13, 136.00, 135.77, 135.49, 135.39, 132.82, 131.21, 130.41, 127.79, 124.70, 121.27, -0.15. $^{19}$F NMR (282 MHz, $CDCl_3$) δ -132.40 (dd). ESI-MS *m*/*z* calculated for $[C_{31}H_{31}BFN_4S_2Si_2]^+$ 609.7, found 609.5.

**Fabrication of the BHJ solar cells and measurements**

All the devices are fabricated by thermal evaporation based on indium tin oxide (ITO) coated glass substrates (90 nm with 26 Ω/sq and 84% transparency, TFD, USA) in a high vacuum multi-source chamber (K. J. Lesker, UK) with a base pressure about $10^{-8}$ mbar. The wafers are cleaned in a sequence of organic solvents and ozone treatment. All the layers are deposited by vacuum sublimation using shadow masks, which is designed for 6×6 substrates with different stacks. One wafer is completed without vacuum pause, which permit constant preparation condition. For deposition on heated substrates, the glass substrates are irradiated by intense halogen lamps. The substrate temperature is not tracked during evaporation but calibrated beforehand. During deposition of all layers, the substrate rotates in the chamber to minimize thickness inhomogeneities across the wafer. Layer thicknesses are tracked with quartz crystal microbalances. The densities used for the organic substances are given below. After the deposition, the devices are encapsulated immediately under nitrogen using epoxy glue and glass lids. The overlap between the ITO anode and the evaporated metal top electrode present the photoactive area of 6.44 $mm^2$ on the samples.

The standard IV measurements are carried out using simulated sun light from a "16S-003-300" solar simulator from SolarLight Company Inc. (USA). The efficiency values are given using the mismatch corrected intensity, which is calculated using the measured simulator spectrum used for the IV measurement as well as the spectral response of the organic solar cell and the Si reference diode (S1337-33BQ, Hamamatsu) used for intensity monitoring of the solar simulator. For the EQE measurements, the device is monitored using a custom-made setup (Oriel Xe Arc-Lamp Apex Illuminator combined with Cornerstone 260 1/4m monochromator, Newport, USA). The output current response is measured by a lock-in amplifier 7256 DSP (Signal Recovery, UK). Absorption measurements are performed in full devices by measuring the light intensity at the illumination side of the sample after reflection at the metal back contact under consideration of vanishing transmission. The reflection characteristics of the evaporated Al contact is taken into account. Two light sources (halogen and deuterium lamps) are used to cover the full spectral range (Avalight-DH-S-BAL, Avantes). Both illumination and collection of the reflected light is accomplished by a quartz glass fiber and analyzed by a CAS 140 spectrometer (Instrument Systems).

**Mobility measurements**

For determining the charge carrier mobility of the materials in this study organic field effect transistors (OFETs) were utilized. Standard bottom-gate-bottom-contact OFET substrates (Frauenhofer IPMS Dresden) were used with channel lengths between 2.5 and 20 μm and channel width of 10 mm. The gate oxide is 230 nm thick $SiO_2$ and the source and drain electrodes consists of 30 nm Au with 10 nm indium tin oxide as adhesion layer. The predefined substrates were cleaned with acetone, ethanol and isopropanol and cleaned in an ultrasonic bath for 5 min each, followed by 10 min oxygen-plasma treatment. Finally, the active organic material was deposited by thermal evaporation at a base pressure of ~$10^{-7}$ mbar, $T_{substrate}$ = 298 K and deposition rate = 0.05 nm/s with

a thickness of 30 nm (thickness monitored by quartz crystal microbalance). From the vacuum chamber the samples were transferred without air exposition to a glovebox $O_2$, $H_2O$ < 6 ppm and mounted to the transistor measurement setup. Electrical characteristics of all devices were measured using a HP 4145B semiconductor parameter analyzer with a connected PC and custom LabView Software. The effective charge carrier mobility $\mu$ of the regarding material within the OFETs was determined by linearly fitting the transfer characteristics in saturation regime of all provided channel lengths (see **Figure S9**) and using the expression

$$\mu_{sat} = \frac{2L}{C_{diel}W}\left(\frac{\partial\sqrt{I_D}}{\partial V_{GS}}\right)^2$$

where $L$ is the channel length, $C_{diel}$ the capacity of the gate dielectric, $W$ the channel width $I_D$ the source drain current and $V_{GS}$ the applied voltage between Gate and Source contact. Afterwards the mean value of $\mu$ for all channel lengths was calculated. Table XXX shows the extracted mobilities for the used materials.

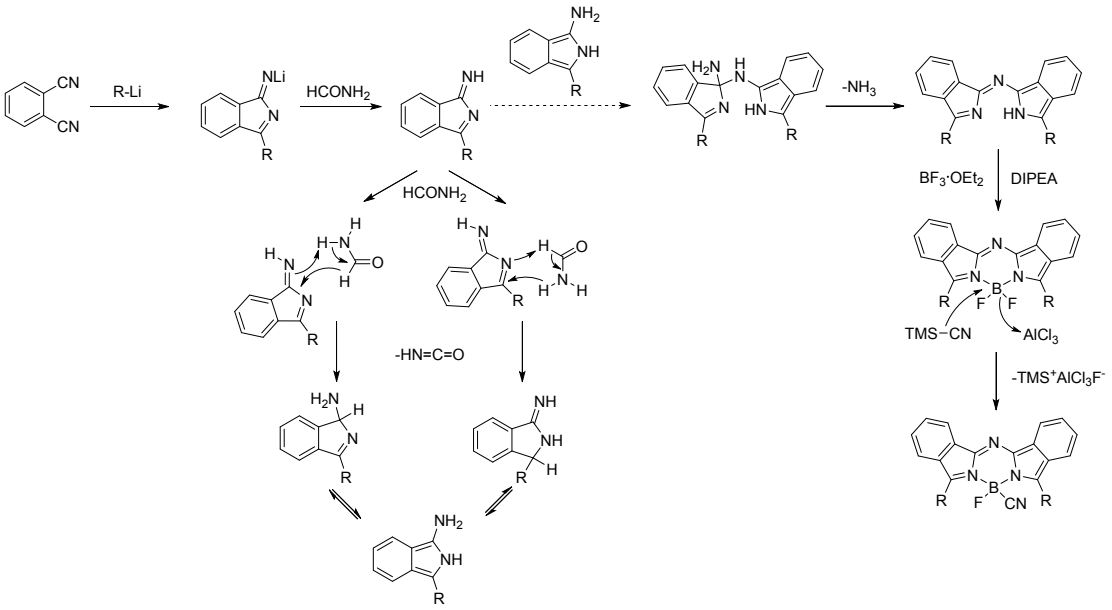


**Scheme S1**. Possible reaction mechanism for the general synthesis of aza-diisoindolmethine precursors, aza-bodipy dyes and derivative.

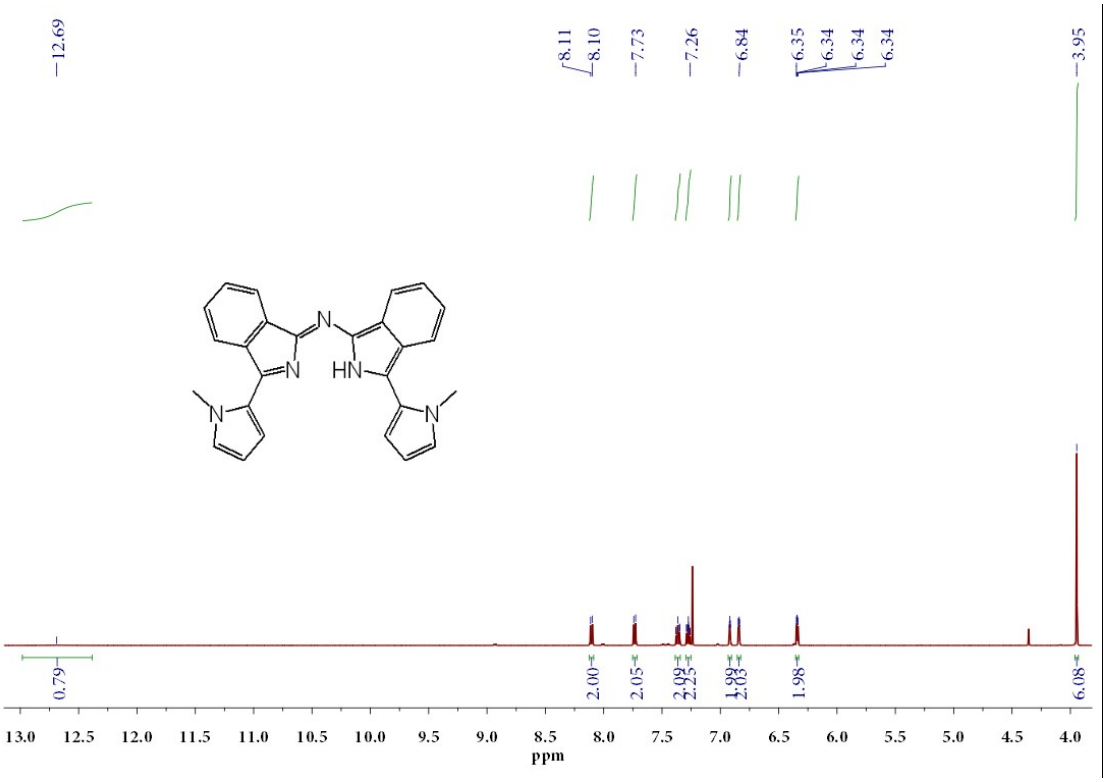
12.69
8.11
8.10
7.73
7.26
6.84
6.35
6.34
6.34
6.34
3.95
N
N
HN
N
N
0.79
2.00
2.05
2.93
2.23
1.98
1.03
1.98
6.08
13.0 12.5 12.0 11.5 11.0 10.5 10.0 9.5 9.0 8.5 8.0 7.5 7.0 6.5 6.0 5.5 5.0 4.5 4.0
ppm

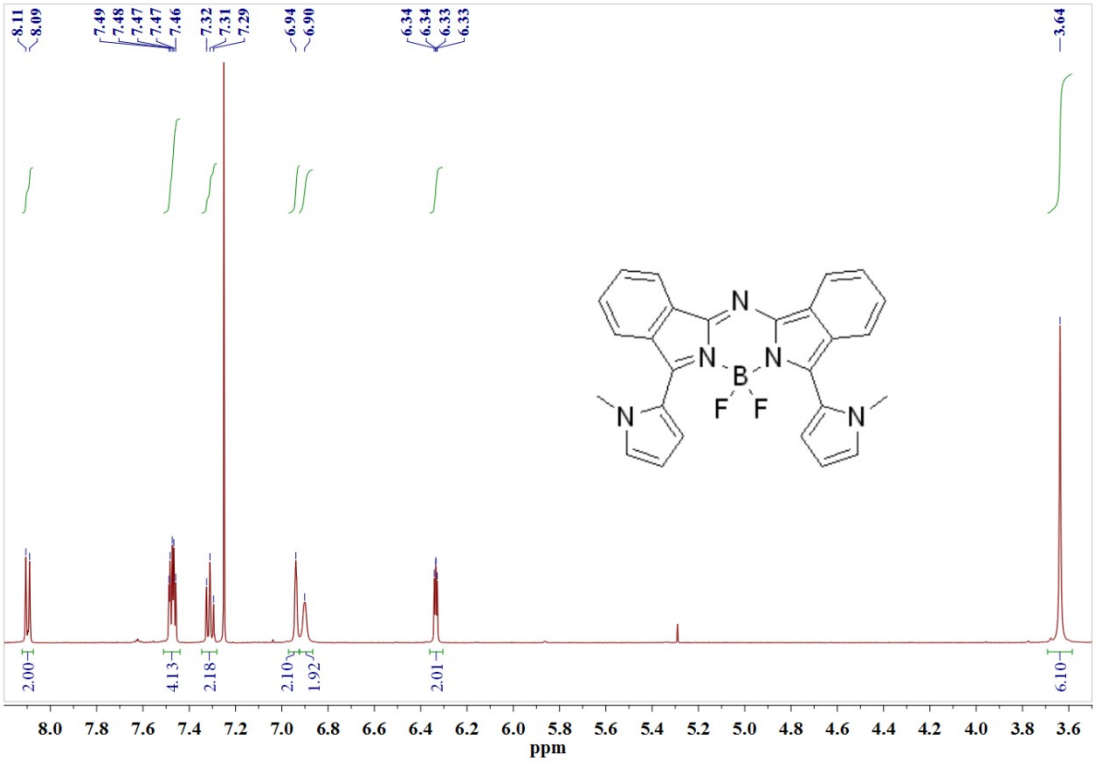
8.11
8.09
7.49
7.48
7.47
7.47
7.46
7.32
7.31
7.29
6.94
6.90
6.34
6.34
6.33
6.33
3.64
N
N
B
N
F
F
N
N
2.00
4.13
2.18
2.10
1.92
2.01
6.10
8.0 7.8 7.6 7.4 7.2 7.0 6.8 6.6 6.4 6.2 6.0 5.8 5.6 5.4 5.2 5.0 4.8 4.6 4.4 4.2 4.0 3.8 3.6
ppm

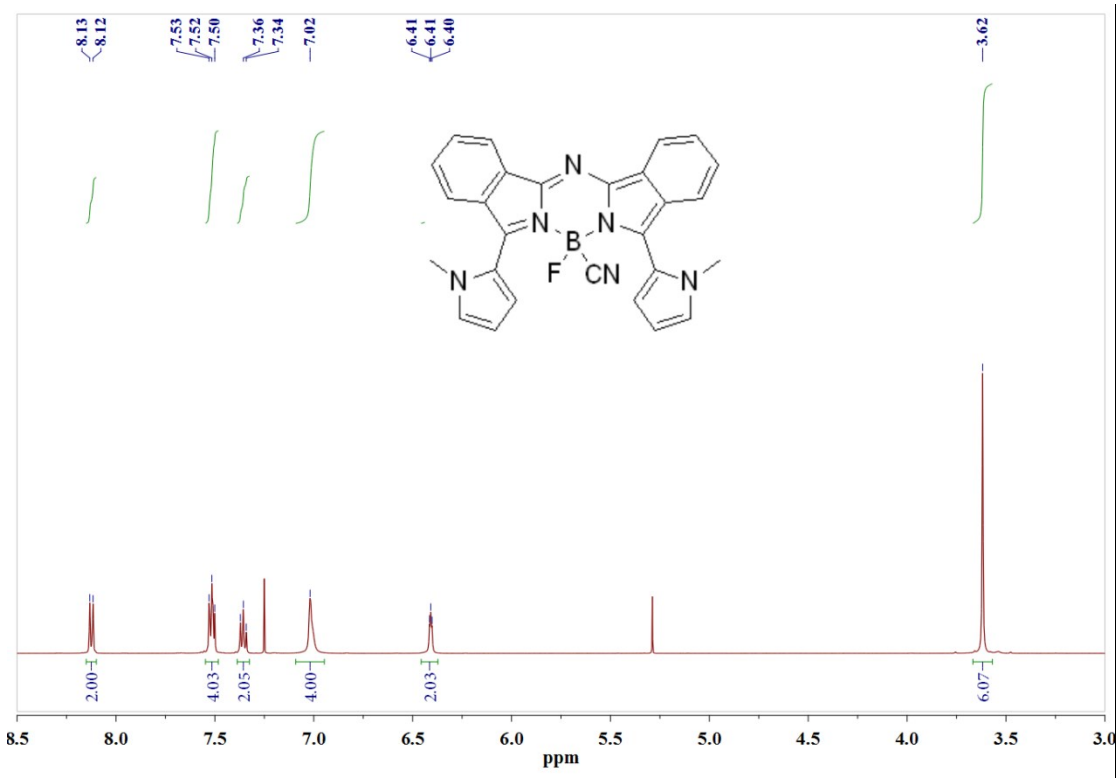
8.13
8.12
7.53
7.52
7.50
7.36
7.34
7.02
6.41
6.41
6.40
3.62
N
N
B
N
F
CN
N
N
2.00
4.03
2.05
4.00
2.03
6.07
8.5
8.0
7.5
7.0
6.5
6.0
5.5
5.0
4.5
4.0
3.5
3.0
ppm

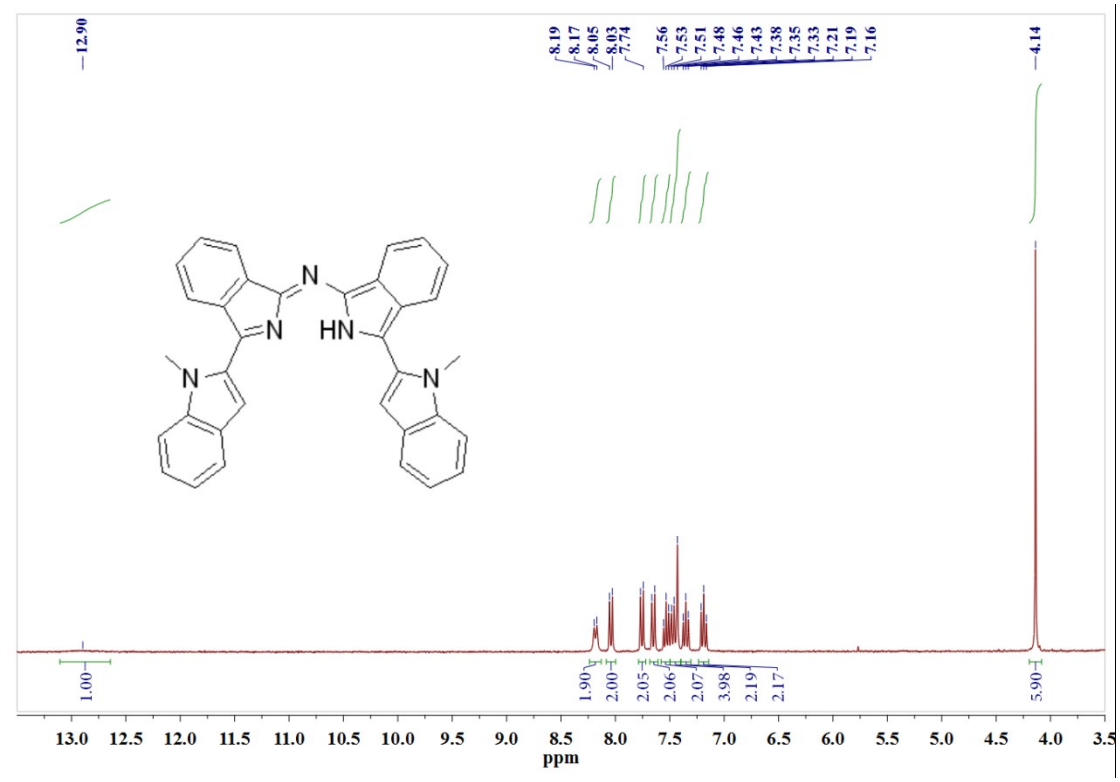
12.90
8.19
8.17
8.05
8.03
7.74
7.56
7.53
7.51
7.48
7.46
7.43
7.38
7.35
7.33
7.21
7.19
7.16
4.14
N
N
HN
N
N
1.00
1.90
2.00
2.05
2.06
2.07
3.98
2.19
2.17
5.90
13.0
12.5
12.0
11.5
11.0
10.5
10.0
9.5
9.0
8.5
8.0
7.5
7.0
6.5
6.0
5.5
5.0
4.5
4.0
3.5
ppm

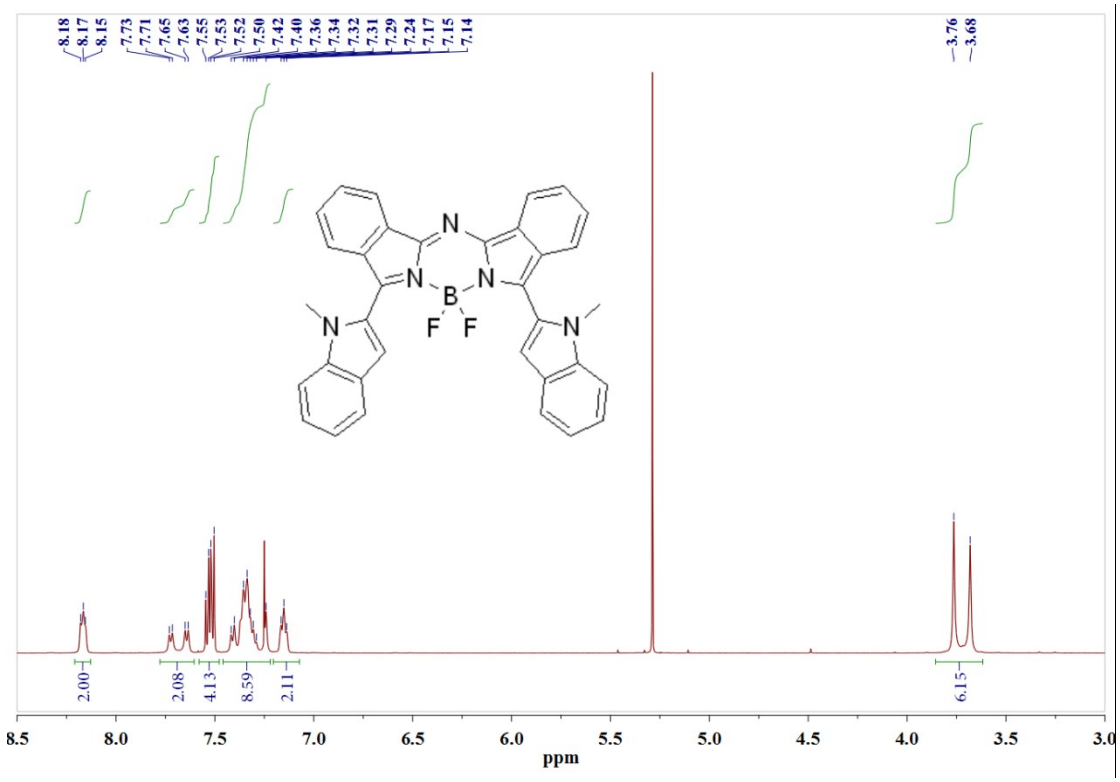
8.18
8.17
8.15
7.73
7.71
7.65
7.63
7.55
7.53
7.52
7.50
7.42
7.40
7.36
7.34
7.32
7.31
7.29
7.24
7.17
7.15
7.14
3.76
3.68
N
N
B
N
F
F
N
N
2.00
2.08
4.13
8.59
2.11
6.15
8.5
8.0
7.5
7.0
6.5
6.0
5.5
5.0
4.5
4.0
3.5
3.0
ppm

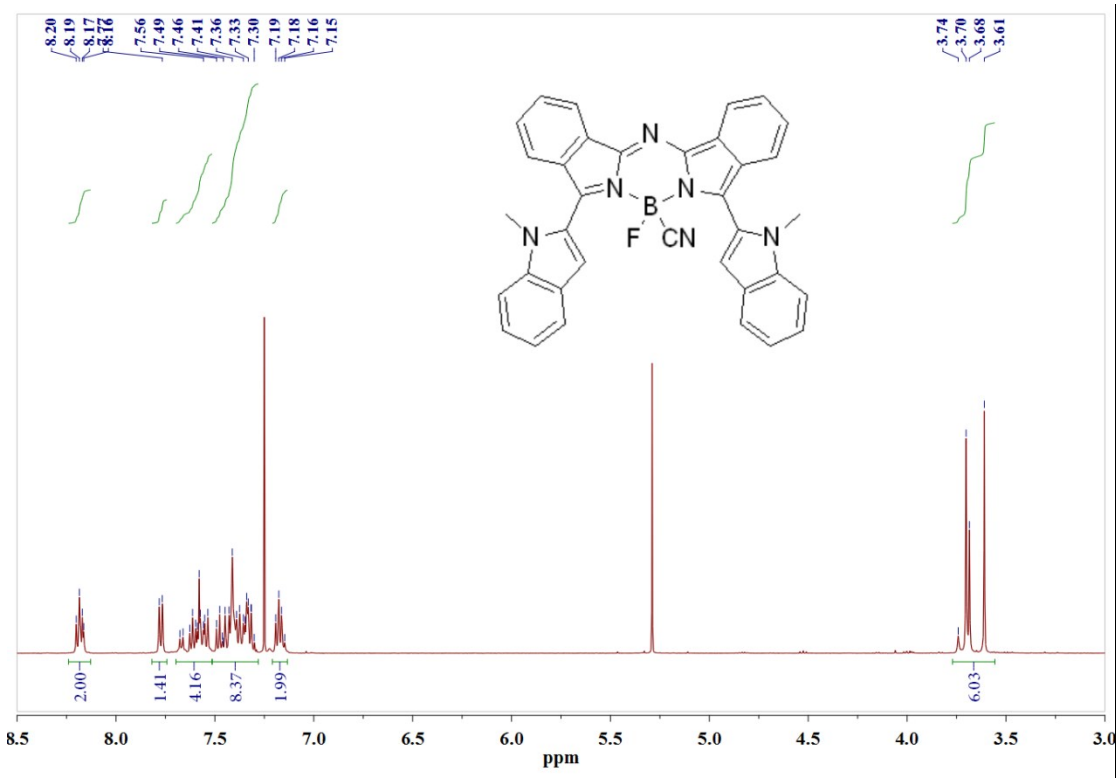
8.20
8.19
8.17
8.16
7.56
7.49
7.46
7.41
7.36
7.33
7.30
7.19
7.18
7.16
7.15
3.74
3.70
3.68
3.61
N
N
B
N
F
CN
N
N
2.00
1.41
4.16
8.37
1.99
6.03
8.5
8.0
7.5
7.0
6.5
6.0
5.5
5.0
4.5
4.0
3.5
3.0
ppm

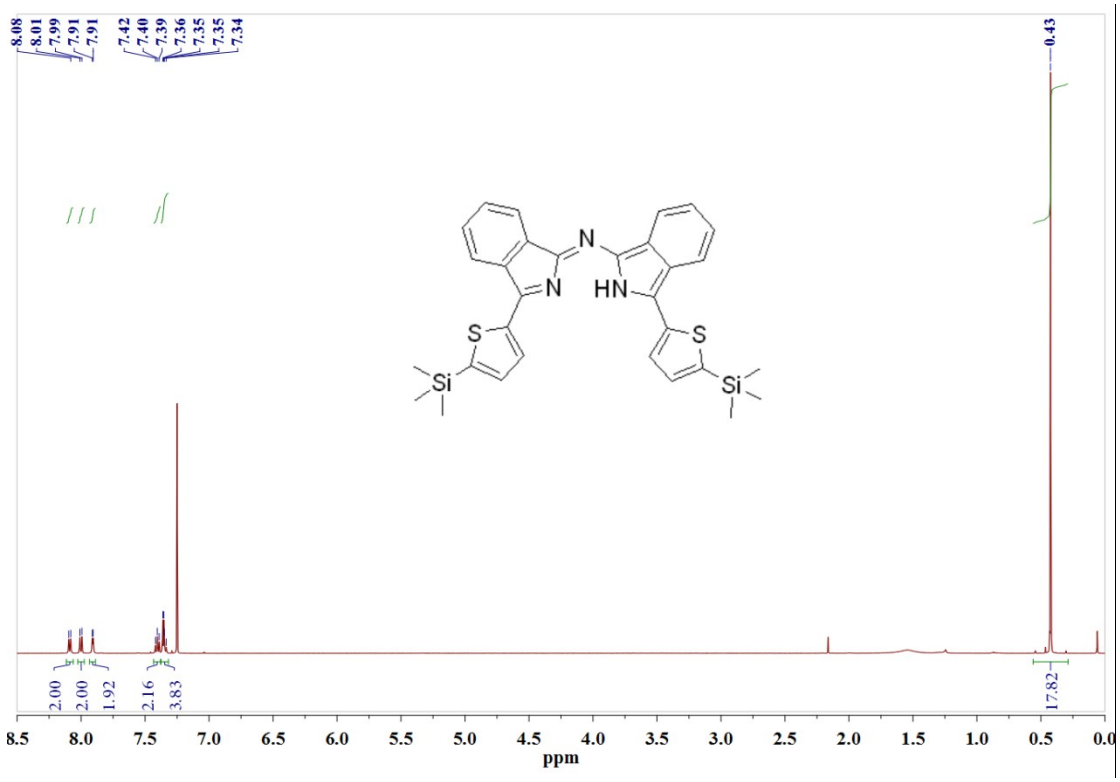
8.08
8.01
7.99
7.91
7.91
7.42
7.40
7.39
7.36
7.35
7.35
7.34
0.43
N
N
HN
S
S
Si
Si
2.00
2.00
1.92
2.16
3.83
17.82
8.5
8.0
7.5
7.0
6.5
6.0
5.5
5.0
4.5
4.0
3.5
3.0
2.5
2.0
1.5
1.0
0.5
0.0
ppm

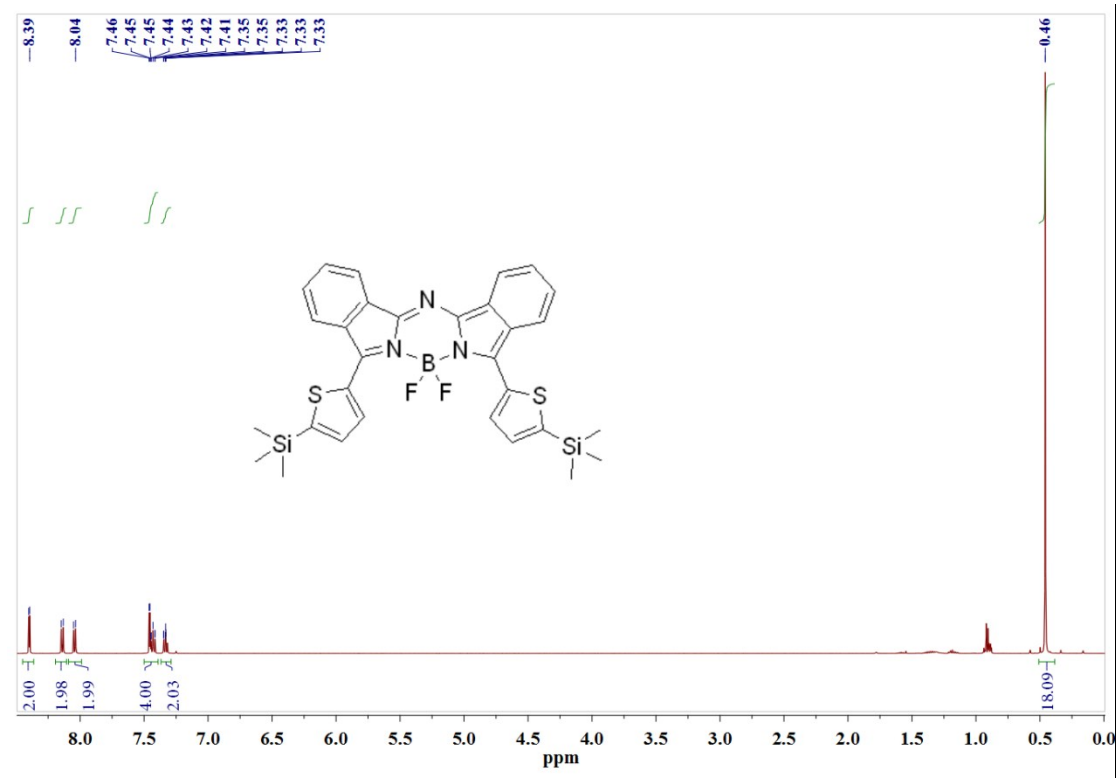
8.39
8.04
7.46
7.45
7.45
7.44
7.43
7.42
7.41
7.35
7.35
7.33
7.33
7.33
0.46
N
N
B
N
F
F
S
S
Si
Si
2.00
1.98
1.99
4.00
2.03
18.09
8.0
7.5
7.0
6.5
6.0
5.5
5.0
4.5
4.0
3.5
3.0
2.5
2.0
1.5
1.0
0.5
0.0
ppm

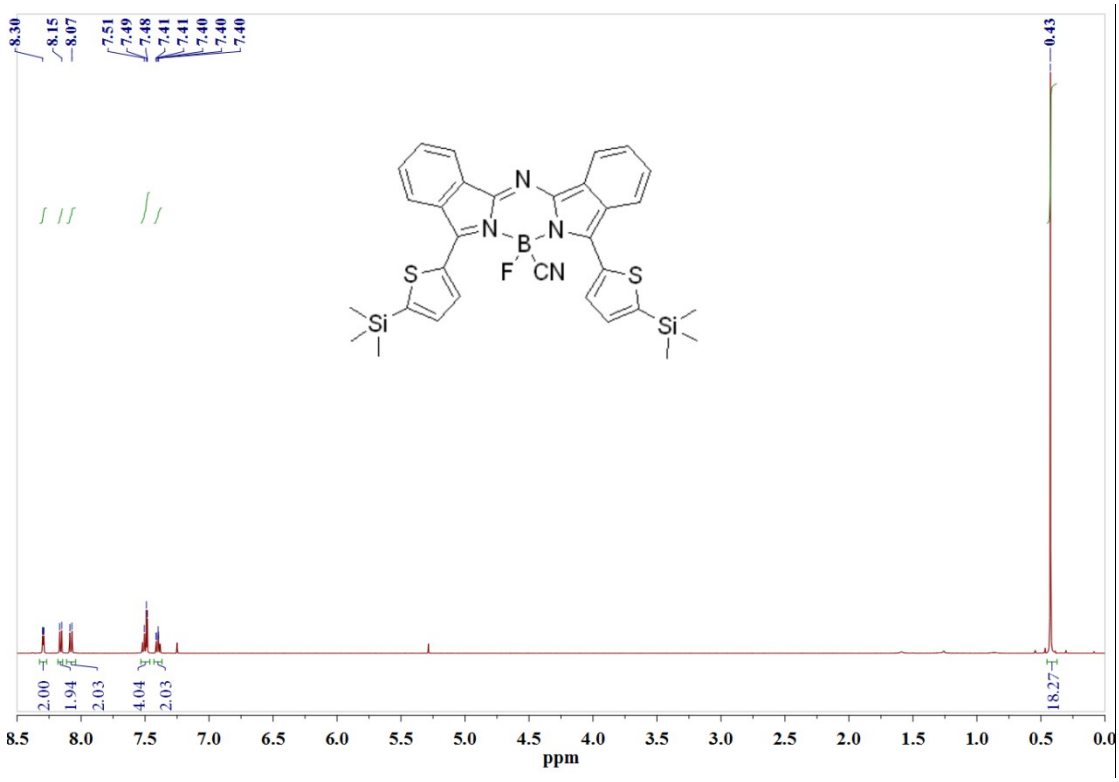


**Figure S1**. The $^{1}$H NMR spectra of compounds **1a**–**3a**, **1b**–**3b** and **1c**–**3c**.

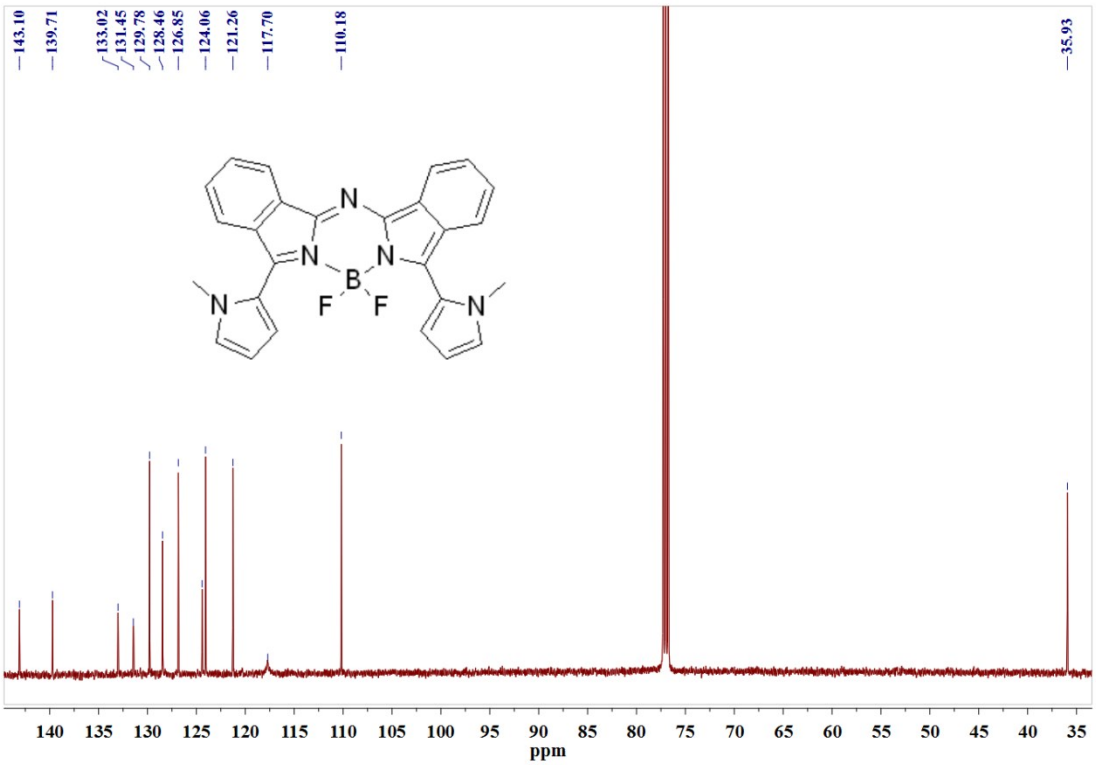
143.10
139.71
133.02
131.45
129.78
128.46
126.85
124.06
121.26
117.70
110.18
35.93
N
N
N
B
F
F
N
N
140 135 130 125 120 115 110 105 100 95 90 85 80 75 70 65 60 55 50 45 40 35
ppm

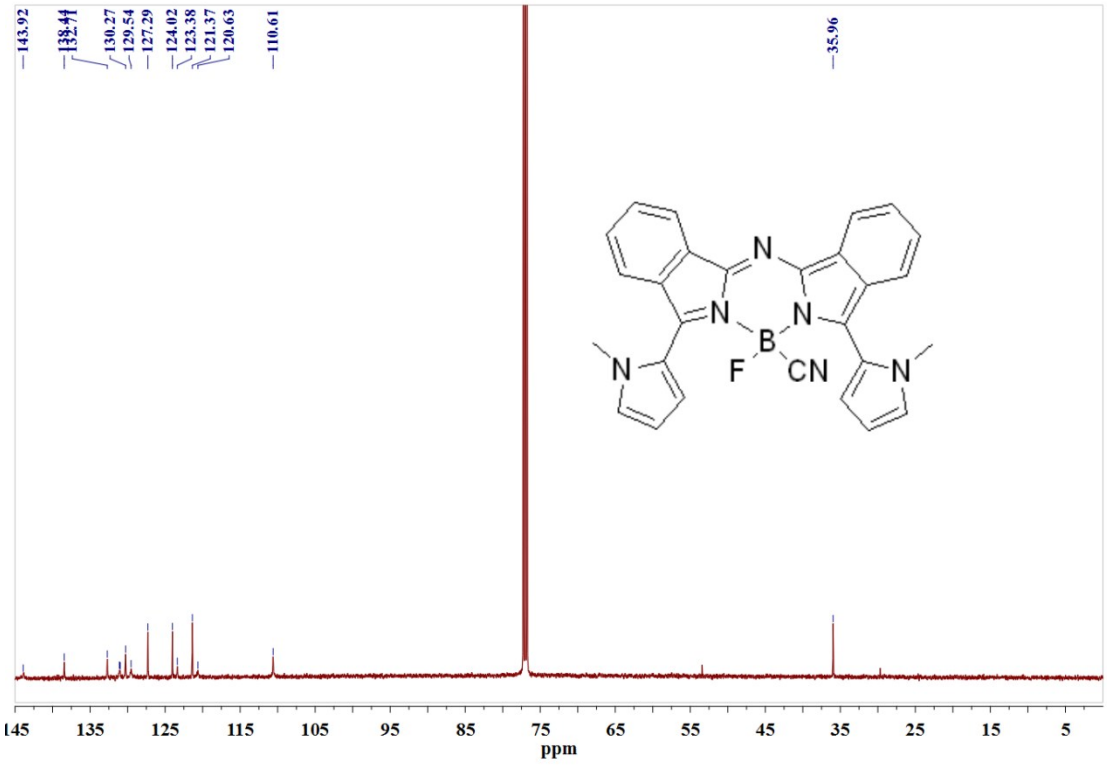
143.92
138.44
132.71
130.27
129.54
127.29
124.02
123.38
121.37
120.63
110.61
35.96
N
N
N
B
F
CN
N
N
145 135 125 115 105 95 85 75 65 55 45 35 25 15 5
ppm

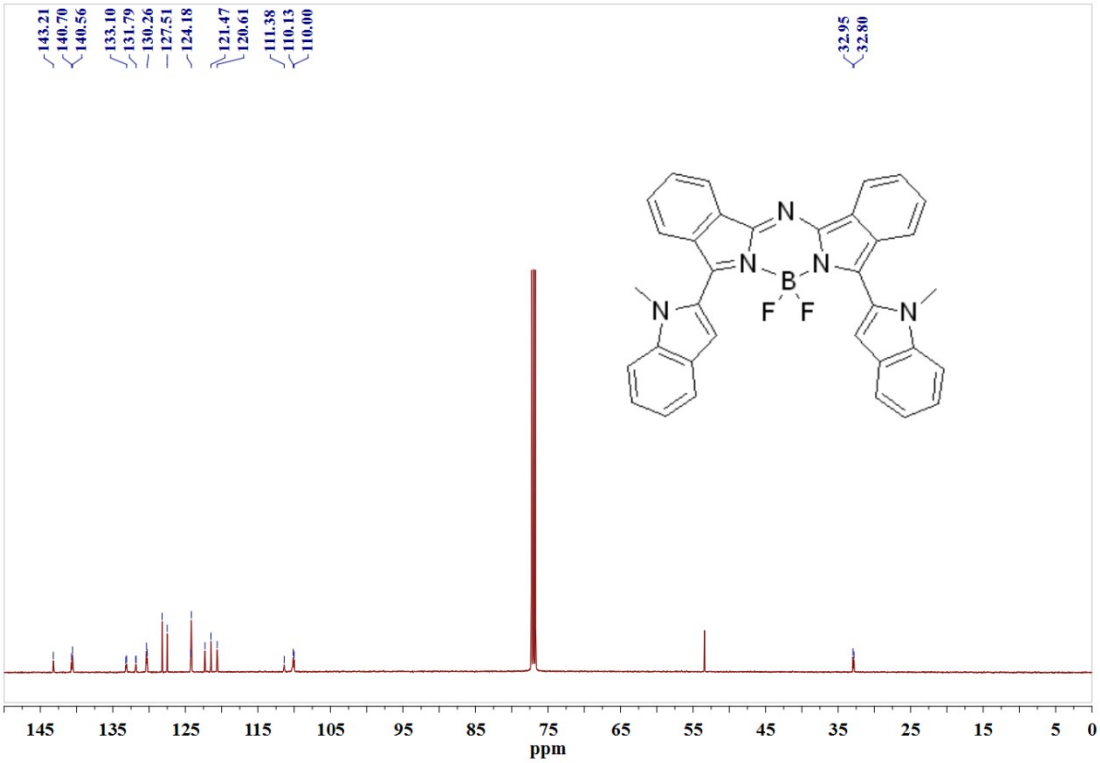
143.21
140.70
140.56
133.10
131.79
130.26
127.51
124.18
121.47
120.61
111.38
110.13
110.00
32.95
32.80
N
N
B
N
F
F
N
N
145
135
125
115
105
95
85
75
65
55
45
35
25
15
5
0
ppm

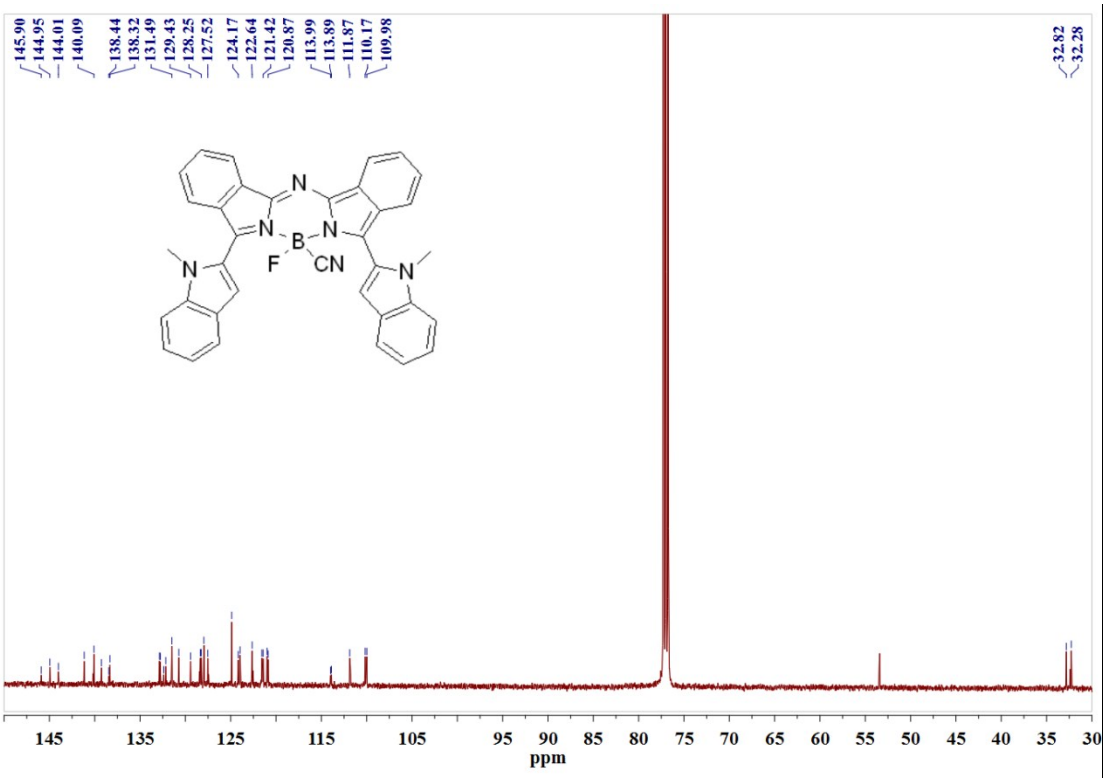
145.90
144.95
144.01
140.09
138.44
138.32
131.49
129.43
128.25
127.52
124.17
122.64
121.42
120.87
113.99
113.89
111.87
110.17
109.98
32.82
32.28
N
N
B
N
F
CN
N
N
145
135
125
115
105
95
90
85
80
75
70
65
60
55
50
45
40
35
30
ppm

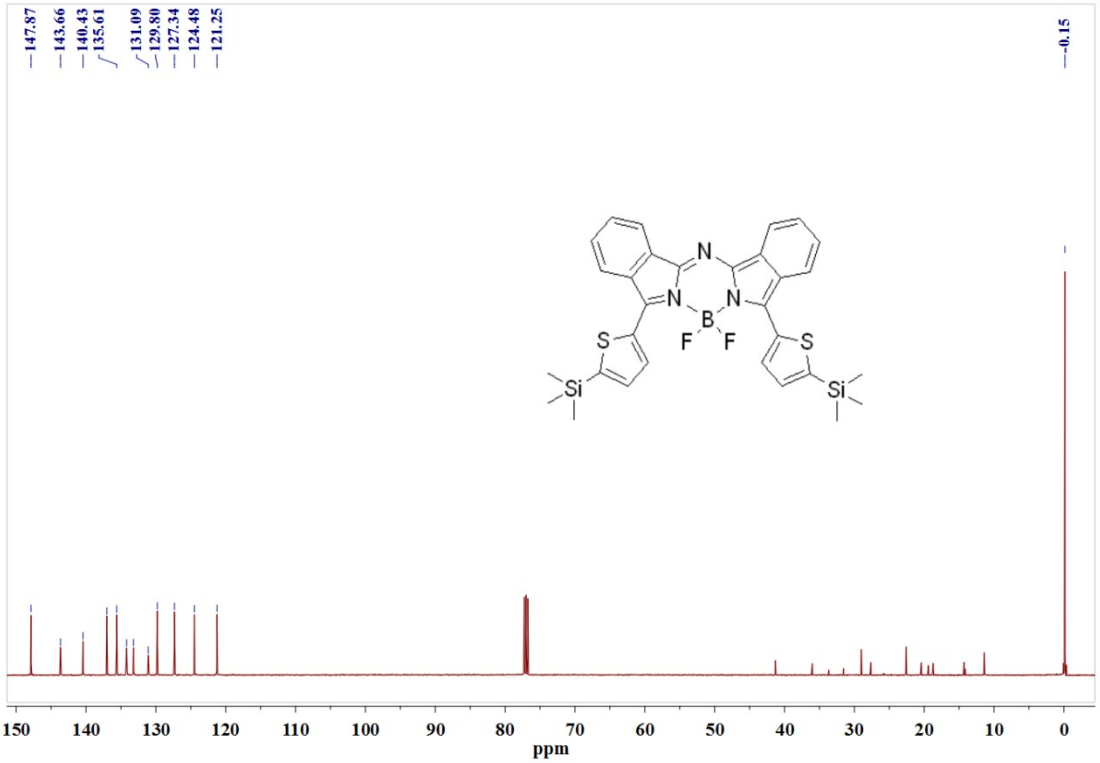


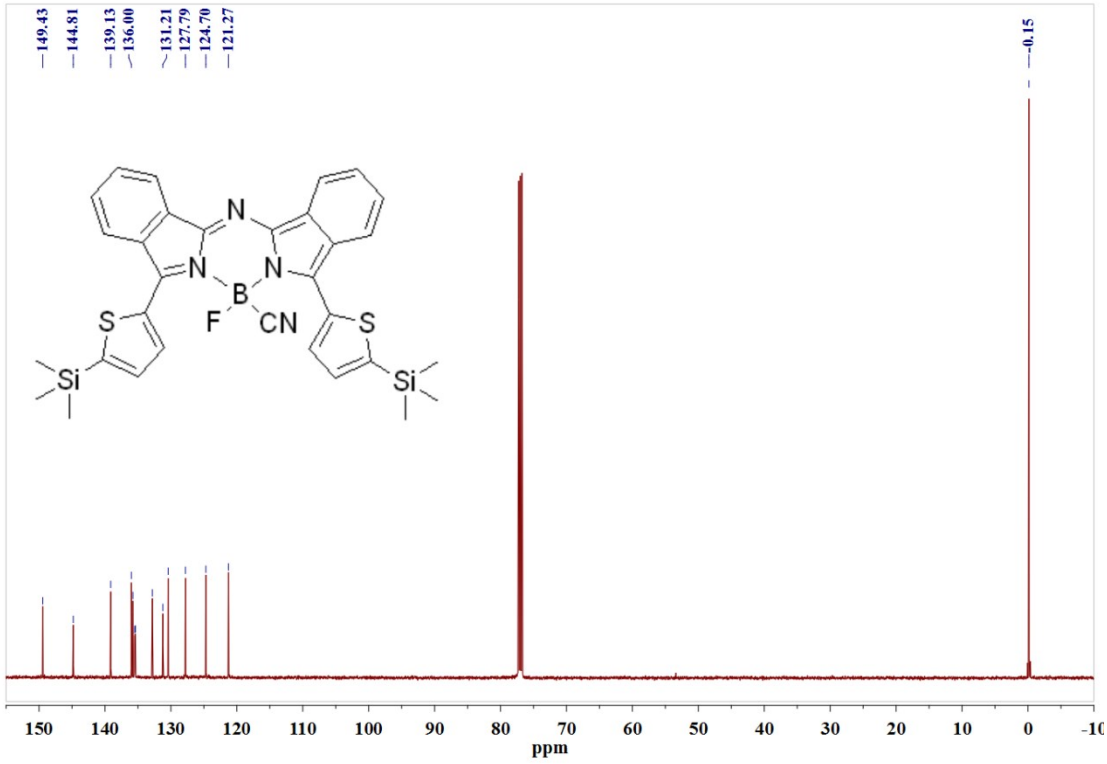


**Figure S2**. The $^{13}C$ NMR spectra of aza-bodipy dyes and their derivatives

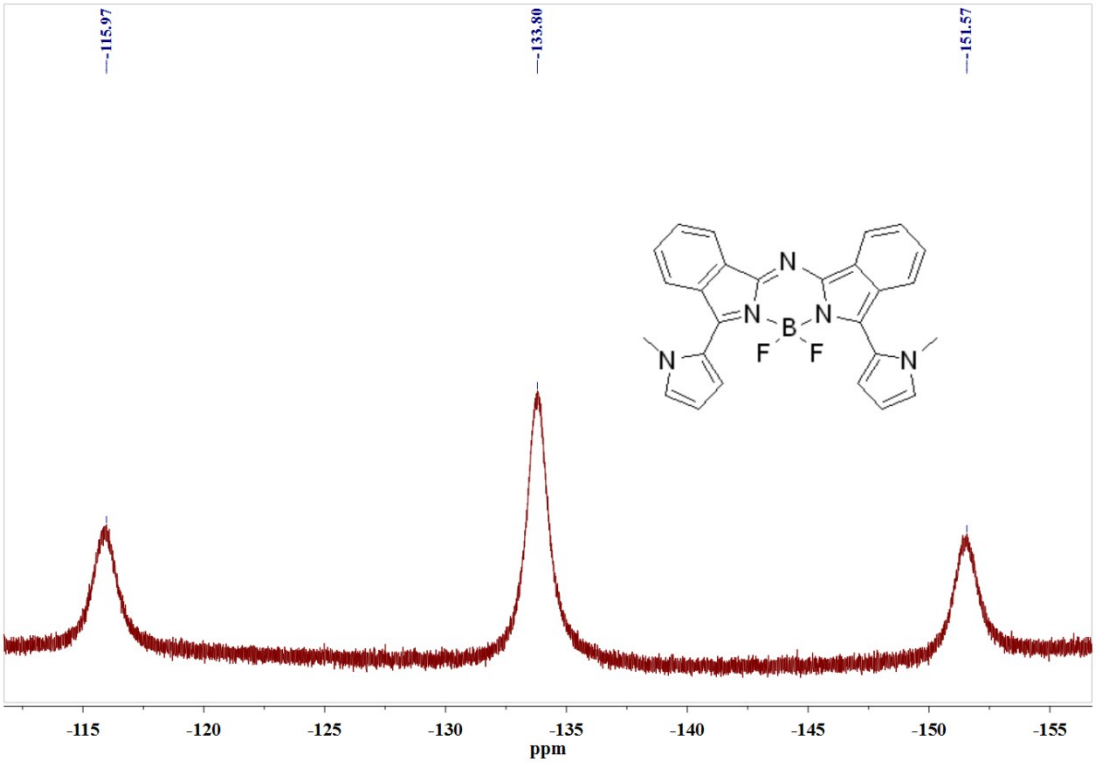
-115.97
-133.80
-151.57
N
N
B
N
F
F
N
N
-115
-120
-125
-130
-135
-140
-145
-150
-155
ppm

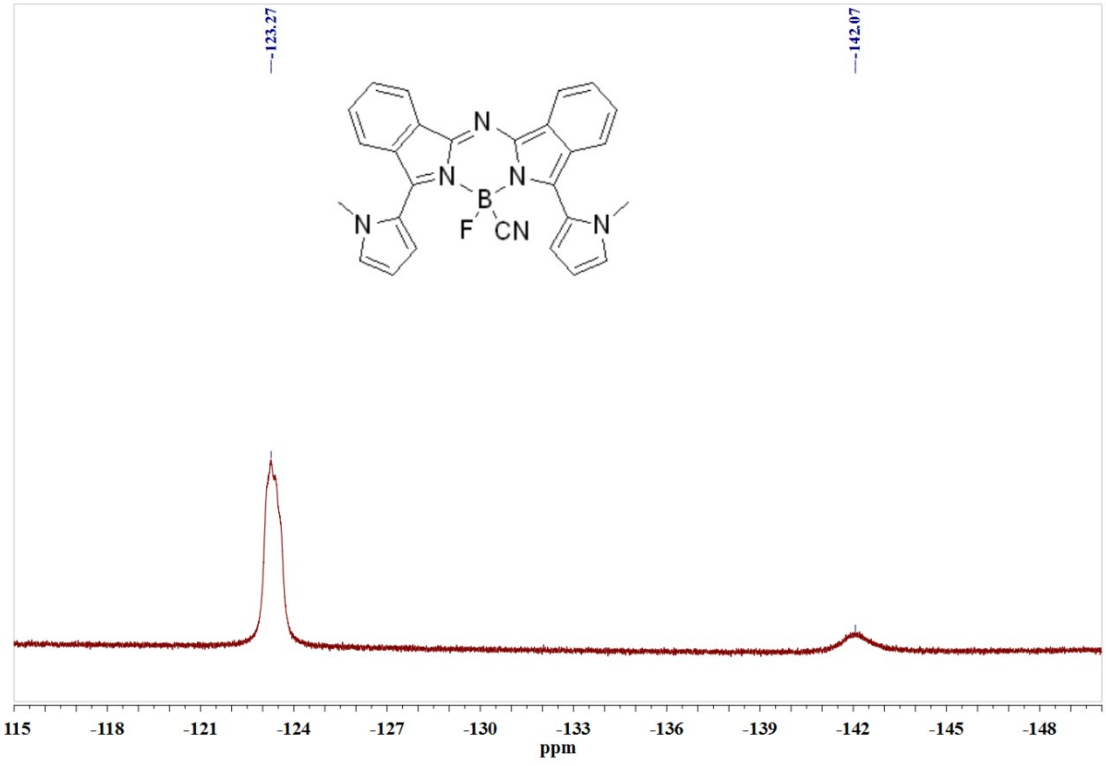
-123.27
-142.07
N
N
B
N
F
CN
N
N
115
-118
-121
-124
-127
-130
-133
-136
-139
-142
-145
-148
ppm

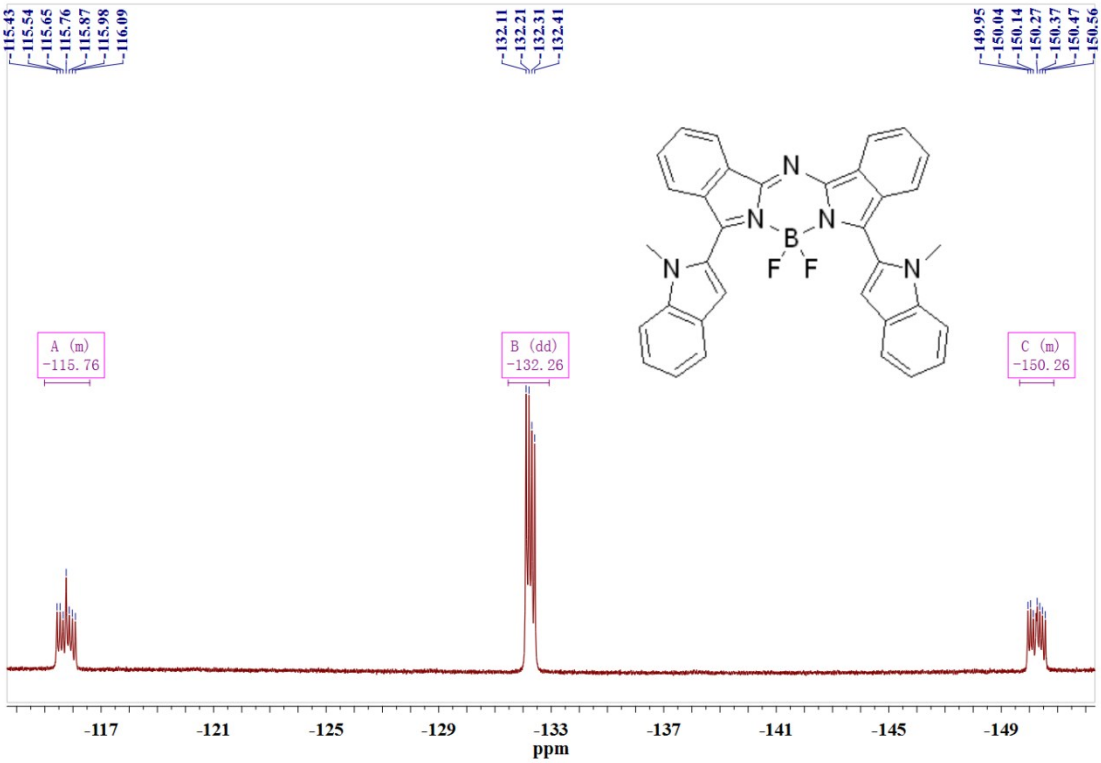
-115.43
-115.54
-115.65
-115.76
-115.87
-115.98
-116.09
-132.11
-132.21
-132.31
-132.41
-149.95
-150.04
-150.14
-150.27
-150.37
-150.47
-150.56
A (m)
-115.76
B (dd)
-132.26
C (m)
-150.26
N
N
B
N
F
F
N
N
-117
-121
-125
-129
-133
-137
-141
-145
-149
ppm

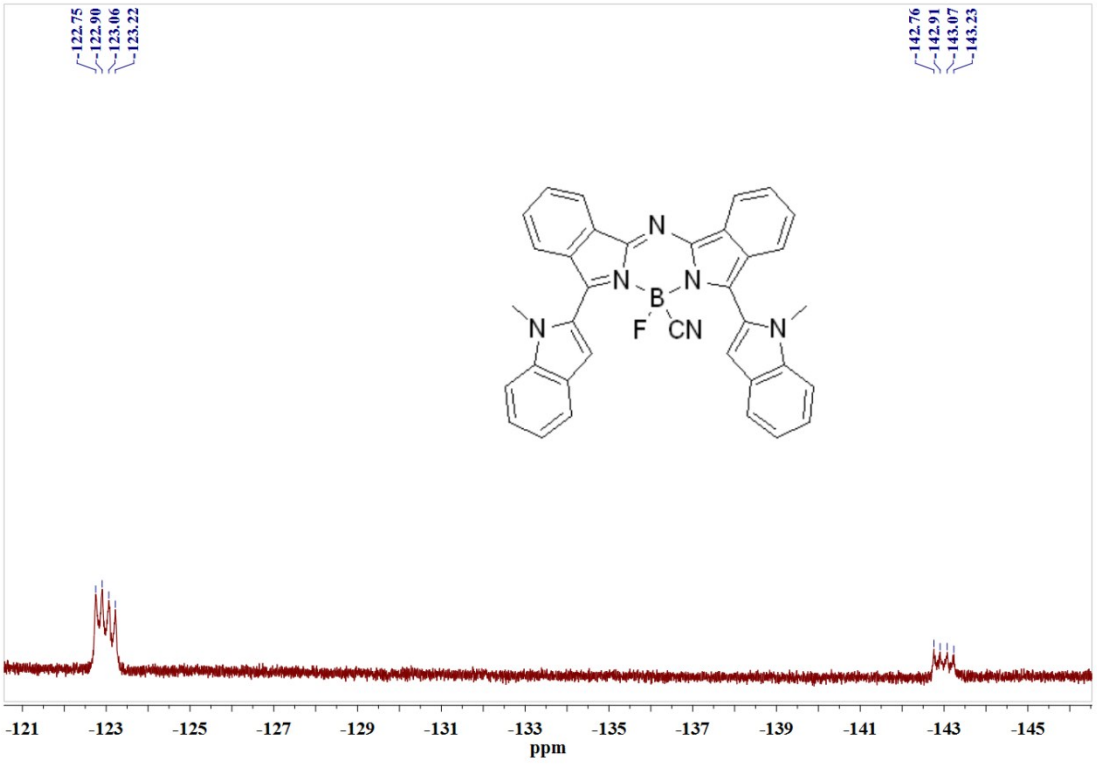
-122.75
-122.90
-123.06
-123.22
-142.76
-142.91
-143.07
-143.23
N
N
B
N
F
CN
N
N
-121
-123
-125
-127
-129
-131
-133
-135
-137
-139
-141
-143
-145
ppm

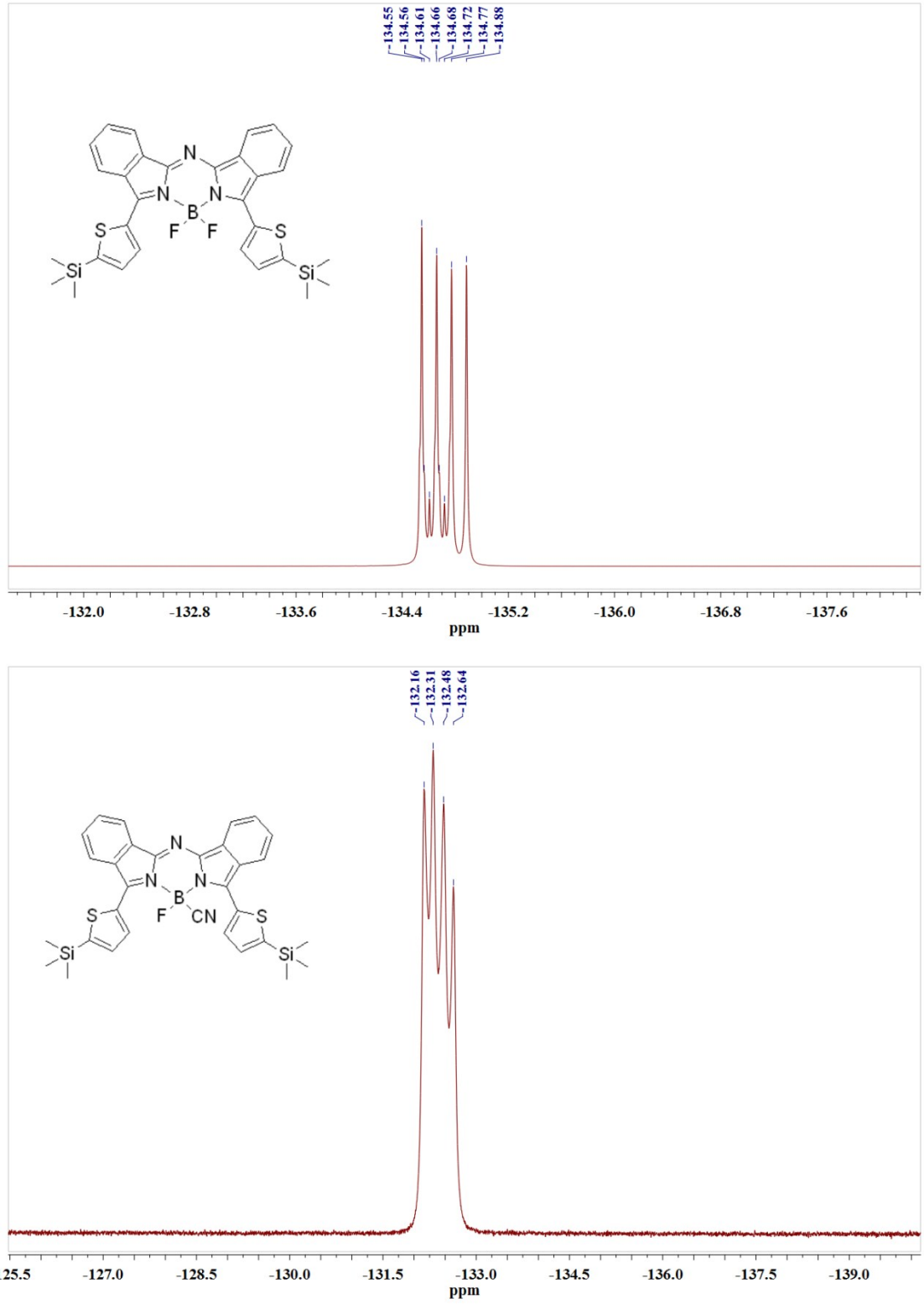


**Figure S3.** The $^{19}F$ NMR spectra of aza-bodipy dyes and their derivatives.

**Table S1.** Crystal data and summary of structure refinements

| Compounds | 1c | 2a | 2b | 3b |
|---|---|---|---|---|
| **Formula** | $C_{28}H_{24}BFN_7$ | $C_{34}H_{25}N_5$ | $C_{34}H_{24}BFN_5$ | $C_{30}H_{30}BF_2N_3S_2Si_2$ |
| **Formula weight** | 488.35 | 503.59 | 551.39 | 601.68 |
| **Temperature [K]** | 200 | 200 | 100 | 200 |
| **Wavelength [Å]** | 0.71073 | 0.71073 | 0.71073 | 0.71073 |
| **Crystal system** | triclinic | triclinic | triclinic | triclinic |
| **Space group** | $P\bar{1}$ | $P\bar{1}$ | $P\bar{1}$ | $P\bar{1}$ |
| ***a* [Å]** | 7.5171(4) | 9.0354(4) | 10.9204(11) | 10.3714(19) |
| ***b* [Å]** | 12.3224(6) | 11.8886(5) | 11.8225(12) | 11.612(2) |
| ***c* [Å]** | 13.2336(6) | 13.4146(6) | 12.8908(13) | 13.514(3) |
| ***α* [deg]** | 89.038(2) | 102.045(3) | 85.313(4) | 104.995(7) |
| ***β* [deg]** | 73.997(2) | 108.397(3) | 73.628(3) | 111.124(6) |
| ***γ* [deg]** | 87.037(2) | 99.521(3) | 65.884(3) | 91.603(7) |
| **Volume** | 1176.73(10) | 1295.03(10) | 1456.4(3) | 1453.1(5) |
| ***Z*** | 2 | 2 | 2 | 2 |
| ***F* (000)** | 510.0 | 528.0 | 572.0 | 628.0 |
| **Unique** | 5684 | 4623 | 6779 | 6984 |
| **Goodness of Fit on *F*2** | 1.054 | 0.923 | 1.046 | 1.034 |
| **Final *R* indices [$I > 2\sigma(I)$]** | $R_1$=0.0646<br>$wR_2$=0.1888 | $R_1$=0.0427<br>$wR_2$=0.0937 | $R_1$=0.0709<br>$wR_2$=0.2122 | $R_1$= 0.0426<br>$wR_2$= 0.1125 |
| **CCDC No.** | 1470373 | 1470374 | 1470375 | 1470376 |

**Table S2.** Selected bond lengths and angles of **1c**, **2b** and **3b**

| | **1c** | **2b** | **3b** |
|---|---|---|---|
| Bond lengths [Å] | | | |
| B-N1 | 1.549(3) | 1.571(3) | 1.559(3) |
| B-N2 | 1.553(3) | 1.556(3) | 1.558(3) |
| B-F1 | 1.380(3) | 1.381(3) | 1.360(2) |
| B-F2 | – | 1.373(3) | 1.373(2) |
| B-C1 | 1.613(4) | – | – |
| Angles [deg] | | | |
| N1-B-N2 | 105.51(18) | 104.75(18) | 106.09(15) |
| F1-B-F2 | – | 111.7(2) | 111.45(17) |
| F1-B-C1 | 110.9(2) | – | – |

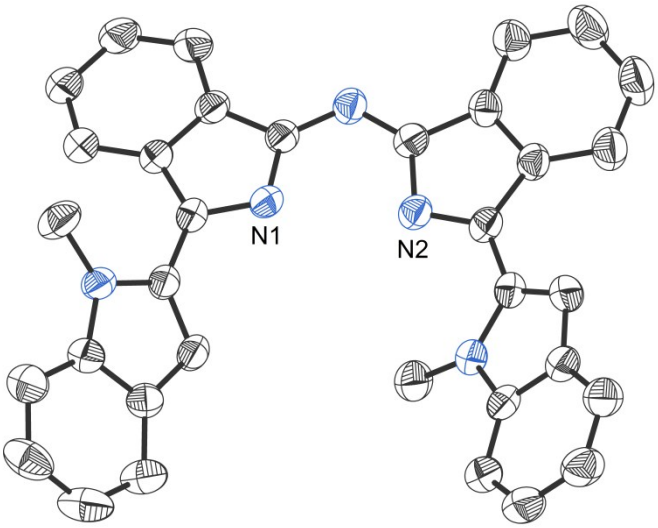


**Figure S4**. The X-ray single crystal structure of **2a**

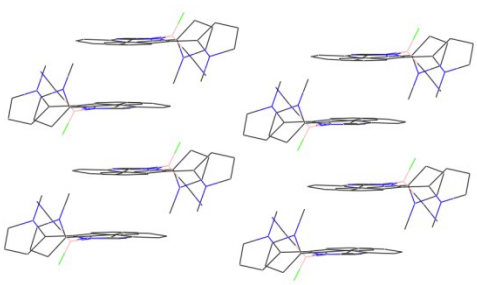

**1c**

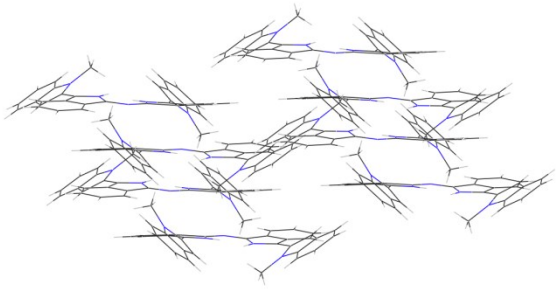

**2a**

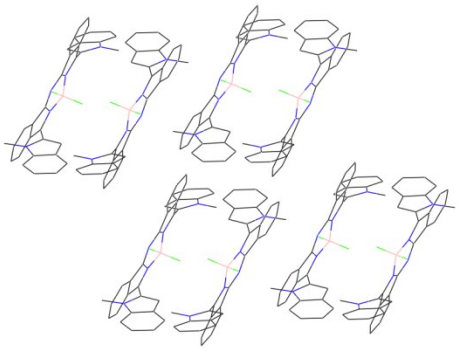

**2b**

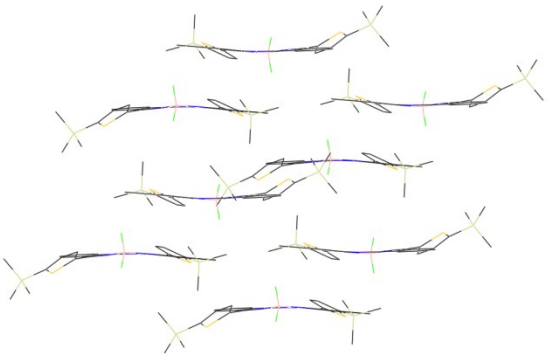

**3b**

**Figure S5**. The packing diagrams of **1c**, **2a**, **2b** and **3b**.

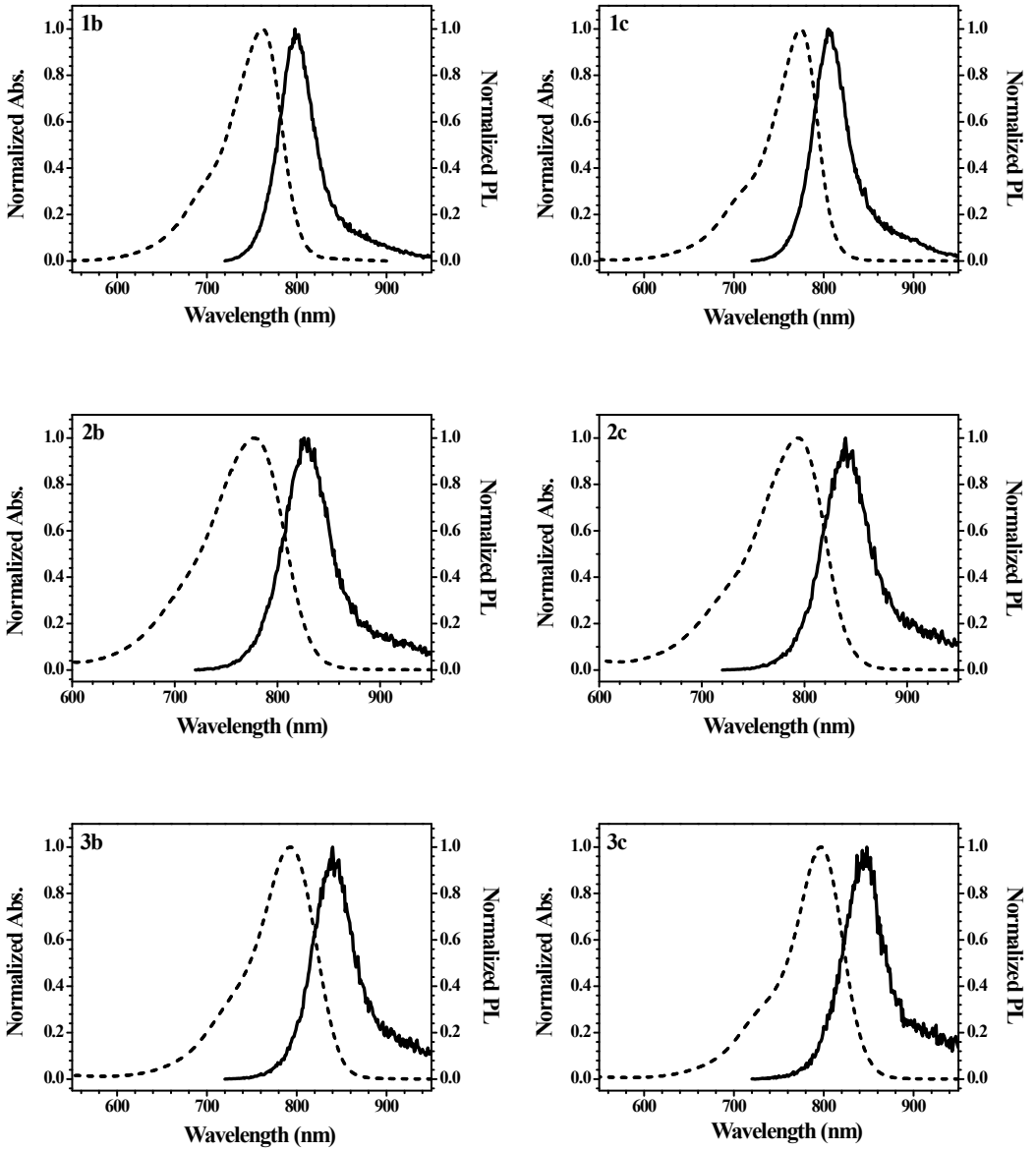


**Figure S6**. The normalized absorption spectra (dash) and emission spectra (solid) of aza-bodipy dyes and their derivatives in DCM solutions at room temperature.

The fluorescent quantum yields were calculated using Rhodamine 101 inner salt whose PLQY was around 0.95 in solution under air as the reference. For each material, five DCM solution samples were prepared with different concentrations. The absorbance intensity at the excitation wavelength was kept lower than 0.1 to avoid reabsorption and inner filter effect. UV-vis spectra and emission spectra of the solutions were recorded at room temperature under air. Then, a plot of absorbance at the excitation wavelength versus the integrated emission area was depicted and the five points for each material was fitted in linear relationship. The gradient of the plot was measured. The PLQY of the unknown sample was calculated according to the equation:

$$\Phi_x = \Phi_{ref}\left(\frac{Grad_x}{Grad_{ref}}\right)\left(\frac{{\eta_x}^2}{{\eta_{ref}}^2}\right)$$

Where $\Phi_x$ and $\Phi_{ref}$ are the PLQYs of the unknown sample and the reference. $Grad_x$ and $Grad_{ref}$ are the calculated gradient of the sample and reference plots. $\eta_x$ and $\eta_{ref}$ are the refractive index of the solvents.

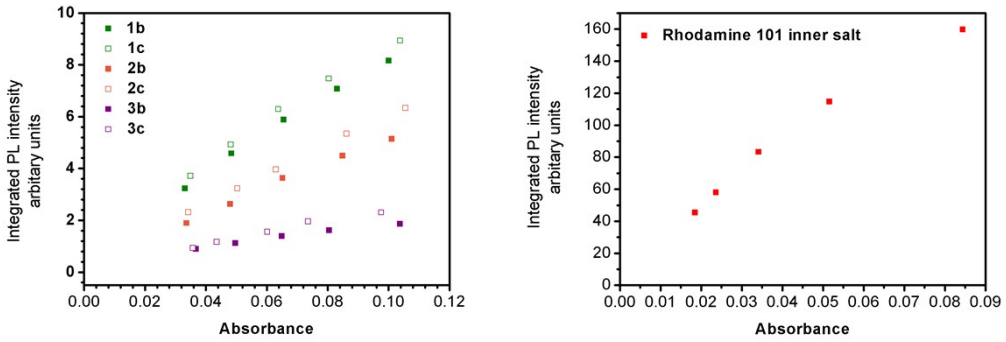


**Figure S7**. The plots of absorbance versus integrated fluorescent emission band of **1b-3b**, **1c-3c** (left) in DCM solution and of Rhodamine 101 inner salt (right) in ethanol solution

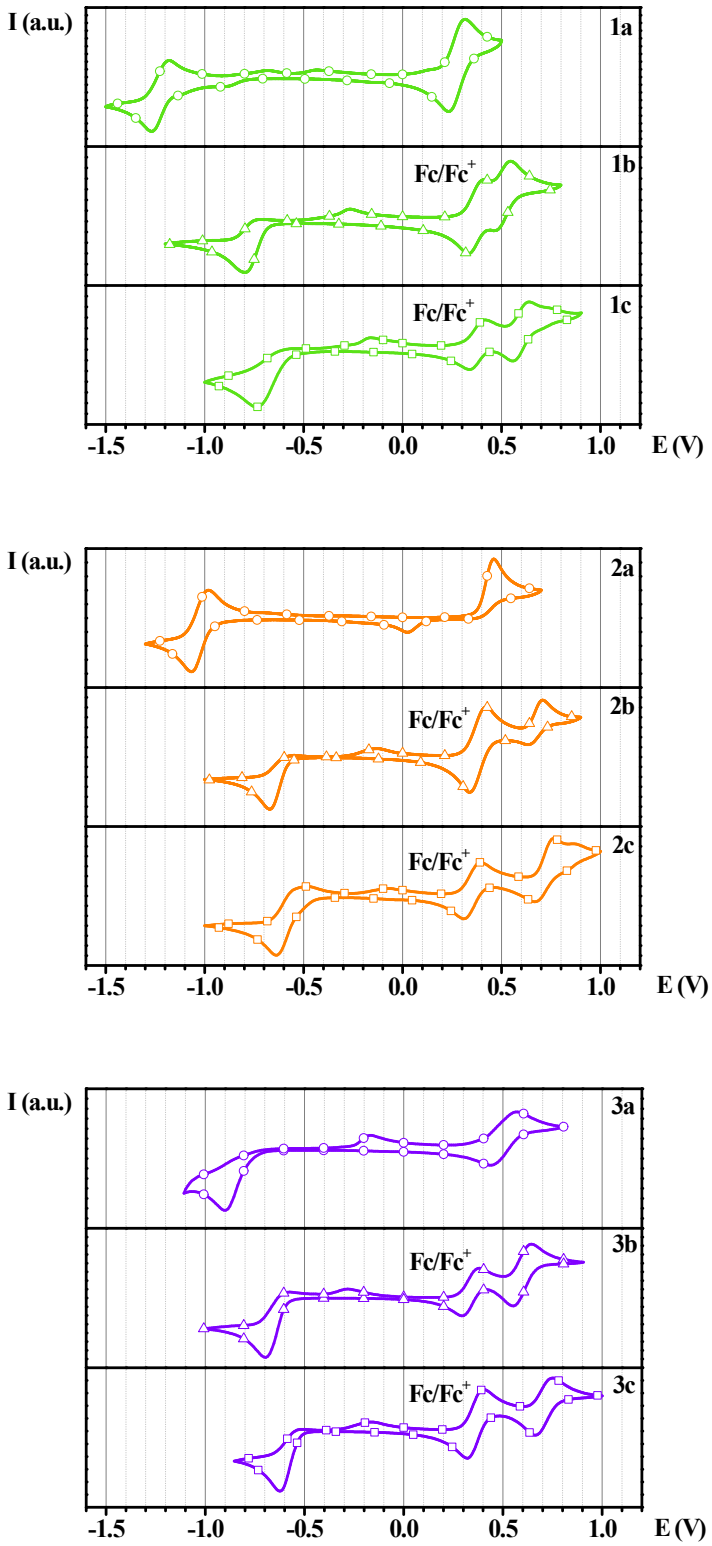


**Figure S8**. The CV plots of all compounds in $1\times10^{-3}$ mol $L^{-1}$ DCM solution. (for aza-bodipy precursors ferrocene is used as external reference and the ferrocene is used as internal reference for aza-bodipy and their derivatives)

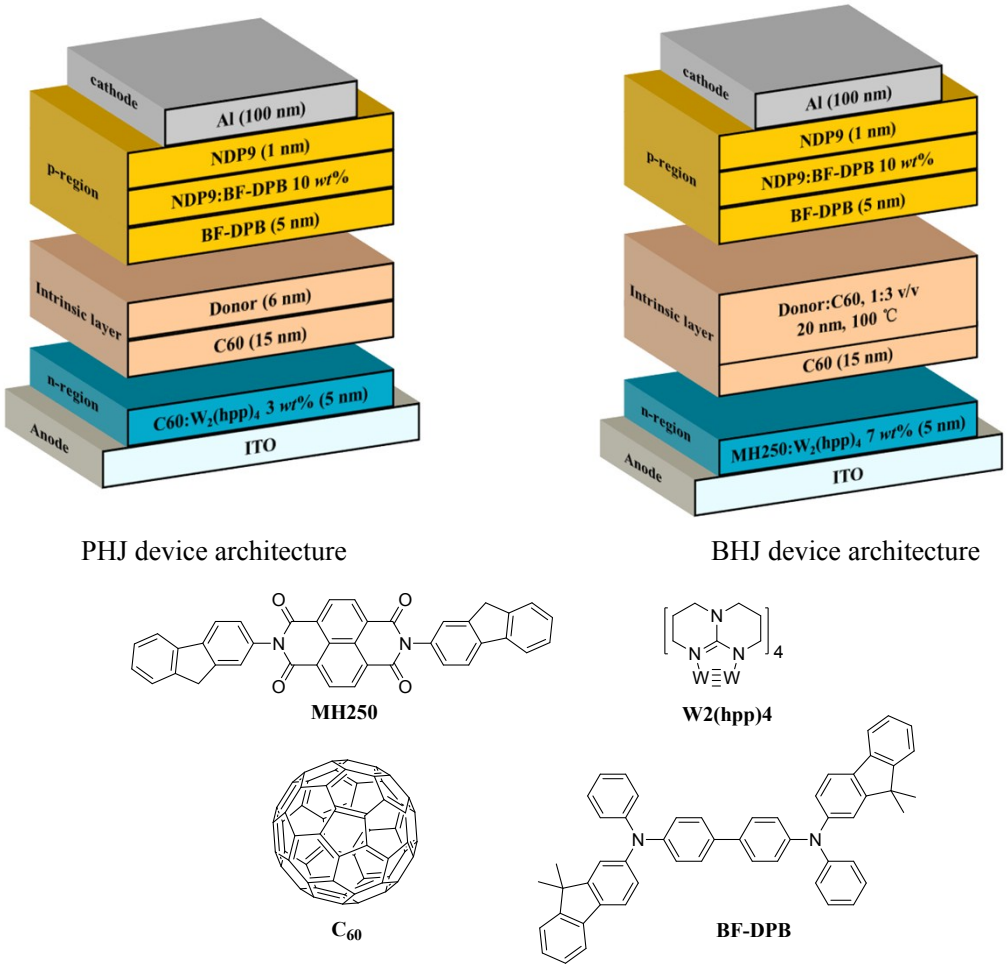


**Figure S9**. The structure of PHJ/BHJ solar cells and the molecular structures of the materials used in the functional layers.

We use high-purity C60 from Creaphys, which is multiply sublimed to reduce impurities. For the layer thickness evaluation during evaporation, we use a material density of 1.63 g/cm$^3$. MH250 was synthesized in house and is used in sublimed grade as well (material density 1.25 g/cm3). BF-DPB is obtained from and sublimed in house (material density 1.21 g/cm$^3$). NDP9 is a commercial dopant purchased from Novaled (Dresden, Germany). The conductivities of the doped layers are in the range of $10^{-4}$ S/cm. Evaporation rates range between 0.03 and 0.06 nm/s for the organic substances and the blend, whereas the metal contact is evaporated at 0.2 nm/s. For all new BODIPY compounds, we assume a density of 1.3 g/cm$^3$.

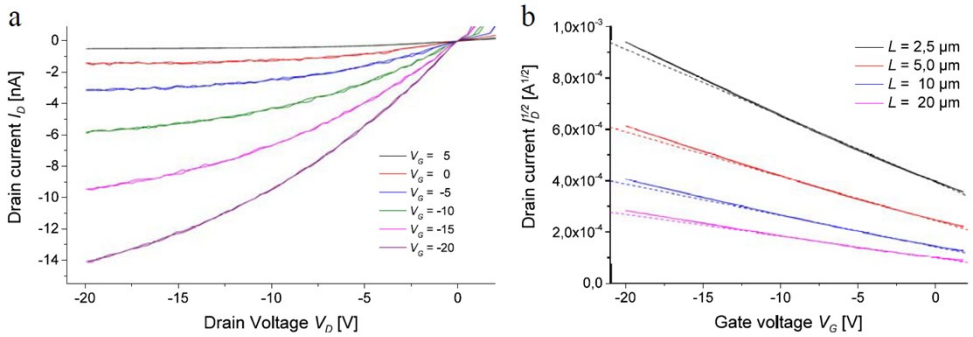


**Figure S10**: Exemplary output characteristic for an OFET with LTY-3 as active organic material at a) with L = 10µm and b) exemplary fits of the transfer characteristics of OFETs with LTY-3 as active organic material ($V_D$ = 20 V) for various channel lengths L. For the fits only gate voltage values from 0 V to -10 V were taken into account since there a saturation of the drain current $I_D$ within the output characteristics was observed.

**Device absorption measurements and estimation of the internal quantum efficiency (IQE)**

Absorption spectra of the pure donor compound deposited on glass can significantly differ from the actual absorption in the device due to morphological effects from mixing with C60, the deposition on heated substrate, the existence of an organic sublayer (here C60 instead of glass) or from interference effects in the thin film stack. Therefore, in order to relate photocurrents to differences in absorption, it is obligatory to measure the real absorption in the device. The setup is described above. Figure S10 shows the absorption spectra of compounds 1b-3b and 1c-3c in PHJ and BHJ devices. We furthermore include the absorption spectrum of the optimized device with higher thickness of the photoactive blend layer.

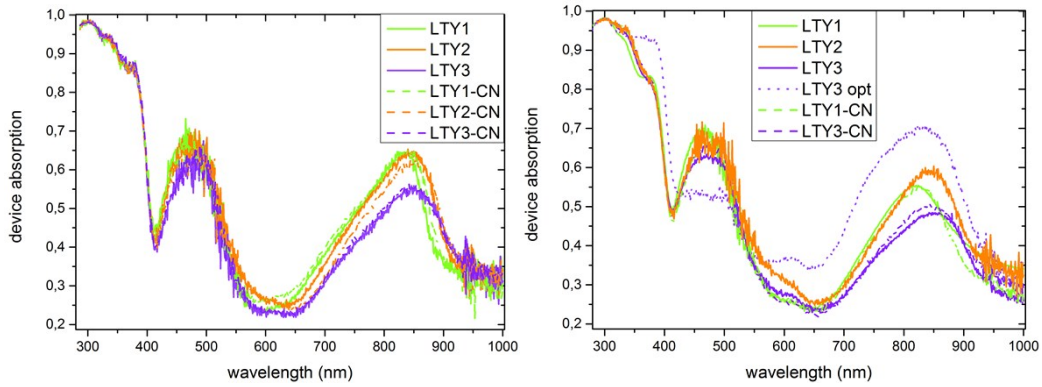


**Figure S11**: Absorption spectra of the PHJ (left) and BHJ (right) devices (including the optimized BHJ device using **3b** as donor) which are described in the main text. The measurement setup is described above. The spectra still contain the parasitic absorption of e.g. the transport layers and the contacts

For the calculation of the IQE, the absorption in the photoactive materials must be extracted. This is usually done by simulating the device absorption based on the optical constants of all materials. As those are not known for the new donor materials, we take the peak absorption of the BODIPY material around 850 nm to calculate the lower limit of the IQE. Although the organic compounds used in the stack do not absorb at wavelengths beyond 750nm, parasitic absorption from the ITO and the metal contact, the doped layers or the reflection at the glass side overlay the actual absorption signal.

Table S3 only shows the lower limits of the IQE as it is difficult to differentiate between the BODIPY absorption and parasitic effects. To give an example: If we reasonably assume that only 10-15% of the incoming light is parasitically absorbed or reflected, the calculation of the IQE of the device containing the blend of **3b**:C60 would return values of 90-100%.

**Table S3**: Estimation of the lower limit of the IQE of donor compounds 1b, 2b, and 3b in PHJ and BHJ devices. For the estimation, we take the measured EQE and absorption values at the peak absorption of the BODIPY material around 850 nm and calculate the IQE using IQE = EQE / Abs.

| donor | PHJ devices | | | BHJ devices | | |
|---|---|---|---|---|---|---|
| | EQE | Abs | IQE (lower limit) | EQE | Abs | IQE (lower limit) |
| **1b** | 0.18 | 0.64 | 0.28 | 0.23 | 0.55 | 0.42 |

| | | | | | | |
|---|---|---|---|---|---|---|
| **2b** | 0.23 | 0.64 | 0.36 | 0.26 | 0.59 | 0.44 |
| **3b** | 0.12 | 0.55 | 0.22 | 0.34 | 0.48 | 0.71 |